Appl. Phys. B 73, 391–399 (2001)
DOI: 10.1007/s003400100714

Applied Physics B
Lasers and Optics

T. VARTANYAN*
J. BOSBACH
F. STIETZ
F. TRÄGER✉

Theory of spectral hole burning for the study of ultrafast electron dynamics in metal nanoparticles

Fachbereich Physik, Universität Kassel, Heinrich-Plett-Strasse 40, 34 132 Kassel, Germany

Received: 12 September 2001
Published online: 15 October 2001 •

ABSTRACT In order to study the ultrafast relaxation dynamics of surface plasmon excitation in metal nanoparticles in the presence of inhomogeneous line broadening and investigate the influence of the reduced dimensions on the dephasing time T_2 in the size regime below about 10 nm, we have recently demonstrated a novel technique based on persistent spectral hole burning [1]. Here, we describe a theoretical model that has been developed for evaluation of the experimental data and precise determination of T_2 for particles of different size and shape. Comparison of the model to experimental data for Ag nanoparticles on sapphire shows that the theoretical treatment does not only reproduce the shape of the generated holes but also the dependence of their widths on the applied laser fluence. As a result, we have a reliable and versatile tool at hand making possible systematic studies of the ultrafast electron dynamics in small metal particles, and the dependence of the femtosecond dephasing time on their size, shape and surrounding dielectric.

PACS 78.66.Bz; 61.46.+w; 71.45.Gm

1 Introduction

Among many other characteristics, the optical properties of nanoparticles, i.e. systems with reduced dimensions, have long attracted special interest in fundamental and applied sciences [2]. In particular, the optical spectra of metal nanoparticles composed of gold, silver or alkali atoms have been investigated quite extensively and are dominated by plasmon polaritons, i.e. collective oscillations of the conduction electrons relative to the lattice of the ion cores that remain at rest. Such excitations can be stimulated with light and give rise to pronounced resonances, the position of which can be varied over a wide spectral range by choosing different metals, by preparing particles of different sizes and shapes and by supporting or embedding them on different substrates or in different matrices. This allows one to tailor novel materials with predetermined special linear and non linear optical properties. Furthermore, excitation of surface plasmons is accompanied by a considerable enhancement f of the local electric field in the vicinity of the nanoparticles [3, 4]. It can be exploited quite profitably to enhance, for example, the photon emission rate of fluorescing species such as dyes or the Raman scattering signal of molecules adsorbed on nanoparticles or on rough metal films [5–7]. This field enhancement is currently being exploited or discussed for applications like all optical switching devices [8], improved biophysical sensors [9] or optical tweezers [10].

While the positions of the resonances of surface plasmon excitation as a function of particle size, shape and dielectric properties are well understood, the ultrafast dynamics of these collective electronic excitations in nanoparticles has remained a highly interesting issue to be elucidated in much greater detail [1, 11–22]. An essential issue is, for example, how rapidly the collective excitations lose their phase coherence [1, 15–17, 19–22]. Further, one would like to investigate the mechanisms responsible for dephasing, i.e. clarify the role of relaxation processes like Landau fragmentation, electron–electron and electron–surface scattering or chemical interface damping [2, 15, 23–25]. For this purpose, study of the influence of the reduced dimensions of the particles, i.e. of confinement of the electrons, and of the surrounding material on the dephasing time T_2 and the relaxation mechanisms is essential. We also note that knowledge of T_2 is important for the applications mentioned above since the enhancement factor f of the electric field near the nanoparticles is directly proportional to T_2; therefore, measurement of this quantity makes possible the experimental determination of f. Detailed understanding of the dependence of the dephasing time on the size and shape of the metal particles would also allow one to optimize f. In short, knowledge of the dephasing time T_2 is essential for basic science and for a large variety of applications. Undoubtedly, however, determination of T_2 constitutes a great experimental and conceptual challenge since typical values are as small as several femtoseconds [1, 15–17, 20–22].

In contrast to the pronounced scientific and applied interest, systematic investigations of $T_2 = 2\hbar/\Gamma_{\mathrm{hom}}$, Γ_{hom} being the homogeneous line width of the resonance, are not available at present. At first glance, one might argue that T_2 can be readily extracted from the widths of the resonances that appear in the absorption spectra of the nanoparticles. In practice, however, the particles usually have broad size and shape distributions. Since the plasmon frequency depends on both

✉ Fax: +49-561/804-4518, E-mail: traeger@physik.uni-kassel.de
Permanent address: Vavilov State Optical Institute, P.O. Box 953, St. Petersburg 197101, Russia. (E-mail: tigran@jamnet.spb.su)

parameters, this introduces inhomogeneous line broadening of the plasmon resonances of such samples. Since the magnitude of the inhomogeneous broadening is not known quantitatively, the homogeneous width Γ_{hom} and the decay time cannot be extracted: the absorption spectra only provide a lower limit of the surface plasmon dephasing time. Furthermore, inhomogeneous broadening also prevents determination of T_2 by time resolved experiments using femtosecond laser pulses and second or third harmonic generation. In such measurements, inhomogeneous line broadening causes narrowing of the recorded autocorrelation traces, an effect that prevents an accurate determination of Γ_{hom} and, at best, allows one to extract an upper limit of T_2 [26, 27].

In principle, the problem of inhomogeneous broadening of the plasmon resonances can be overcome by fabricating very narrow size and shape distributions, for example using lithographic techniques [20, 21] or, alternatively, by measuring characteristics of single nanoparticles [16, 17, 22]. Both approaches, however, are limited at present to rather large aggregates with diameters above about 40 nm, dimensions at which no influence of the reduced size of the nanoparticles on the decay of the collective excitation is expected [2, 24, 25].

Recently, we have developed a novel technique based on persistent spectral hole burning that allows us to investigate nanoparticles in the particularly interesting size regime below about 10 nm and determine the surface plasmon dephasing time with high accuracy even in the presence of inhomogeneous broadening [1]. For evaluation of the experimental data and extraction of T_2 a theoretical model has been developed. Presentation of this model together with its experimental verification for the case of silver nanoparticles supported on sapphire substrates is the subject of the present paper. The theoretical treatment does not only describe the hole burning process in detail but also quantitatively reproduces the shape of the generated holes and the dependence of their widths on the applied laser fluence. Altogether, we have developed a reliable and versatile tool for systematic studies of the ultrafast electron dynamics in small metal particles, and its dependence on their size, shape and surrounding dielectric.

2 Method of persistent spectral hole burning

Among the variety of non linear optical techniques that do not suffer from inhomogeneous line broadening, hole burning is the most universal and simplest to implement in the case of resonances that exhibit ultrashort decay times. Before describing in detail the theoretical model, the basic principle of hole burning in the absorption profile of an ensemble of metal nanoparticles will be recalled briefly. The idea of our method is as follows, Fig. 1. In a first step, nanoparticles with a broad size distribution are prepared on a transparent substrate by deposition of metal atoms with subsequent surface diffusion and nucleation, i.e. Volmer–Weber growth, Fig. 1a. After measuring their optical absorption spectrum, the nanoparticles are irradiated with nanosecond laser pulses, the photon energy being located within the inhomogeneously broadened absorption profile and the spectral width of the light being negligibly small as compared to the homogeneous and inhomogeneous line broadening, Fig. 1b. In the particles the absorbed photon energy is rapidly converted into heat [11–13]. The fluence of the light is chosen such that the resulting temperature increase of the particles is sufficiently high to stimulate evaporation and/or surface diffusion of atoms [28]. As a result, the size and shape of the nanoparticles interacting with the light change, i.e. a hole is burnt into the absorption profile, Fig. 1c. Finally, the optical spectrum is measured a second time and subtracted from the spectrum of the particles as grown to determine the width of the hole, i.e. Γ_{hom} and T_2.

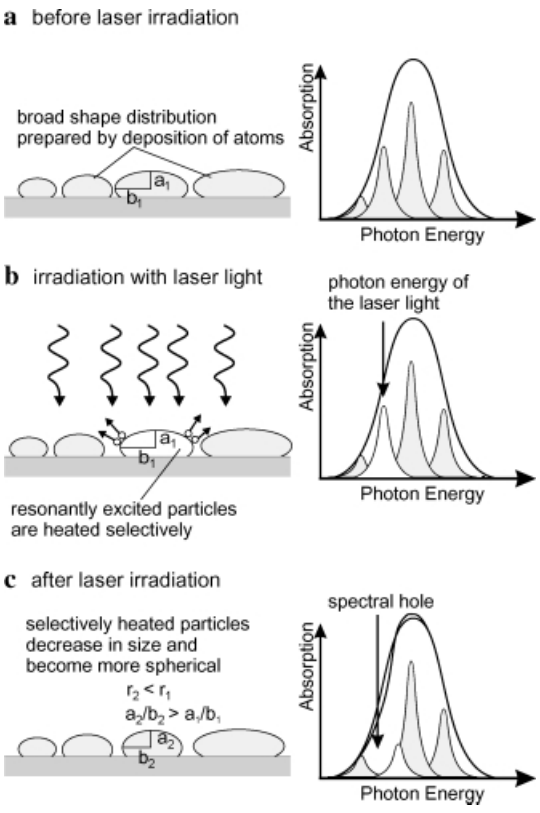

FIGURE 1 Schematic representation of persistent spectral hole burning in inhomogeneously broadened surface plasmon absorption profiles of metallic nanoparticles. Particle distribution and optical spectra **a** before **b** during and **c** after laser irradiation

In such experiments, two different kinds of hole burning have to be distinguished. Very small clusters with sizes below about 1 nm resemble spheres which display a single plasmon resonance and the inhomogeneous line broadening is entirely due to quantum size effects [2, 15]. Larger particles, however, are oblate and can be described as rotational ellipsoids with two main axes a and b, Fig. 1 [28, 29]. The axial ratio a/b is a measure of the shape while the mean radius $\langle r \rangle$, i.e. the radius of a sphere with the same volume as the actual clusters, characterizes their size. a/b drops off as a function of the radius, i.e. there is a correlation between size and shape [28, 29]. For such particles the surface plasmon frequency is essentially size independent; it splits, however, into two modes, the frequencies of which depend on a/b [30, p. 141 ff.]. As a result, the inhomogeneous line width for such deformed nanoparticles is determined mainly by the shape distribution and hole burning in this regime depletes the population of nanoparticles within a certain interval of axial ratios. This makes it possible to selectively excite aggregates with different a/b

values by changing the photon energy and thus study T_2 as a function of cluster shape. In fact, there is a twofold change of the resonantly excited clusters. First, since atoms are preferentially released from the edges and perimeters of the clusters, their long axis b shrinks predominantly, making the clusters more spherical and increasing their plasmon frequency. Secondly, since material is being removed, the particle volume decreases and the amplitude of the plasmon drops off, Fig. 1. In addition, surface self-diffusion may contribute to the shape changes although it does not change the particle volume.

Spectral hole burning is, of course, a well-known technique in atomic, molecular and solid state physics (see, for example, [31, 32]). There is, however, an essential difference of the "classical" experiments as compared to the application described here. In the present case, the "final" state, i.e. the size and shape of the particles after interaction with light, is close to the initial dimensions of the clusters as grown. The nanoparticles change size or shape only until they do not interact with the laser light any more. As a result, an adjacent peak accompanies the hole making its profile asymmetrical (Fig. 1c), a feature that naturally called for the development of the model presented here including an analytical expression of the line shape.

The technique of spectral hole burning as outlined above has a number of advantages, the most essential ones being that it is not restricted to certain particle sizes, does not require special size and shape distributions and is compatible with ultra high vacuum (UHV) conditions, i.e. it allows one to control and systematically vary the chemical environment. Furthermore, there is no need for ultrashort laser pulses with rise times and pulse widths in the femtosecond regime. Since the hole burning process is thermally activated, the most essential parameter is the energy deposited in the particles; therefore, use of laser pulses with several nanoseconds duration and fluences on the order of several tens of mJ/cm^2, which are readily delivered by standard laser systems in the visible and infrared range, is sufficient to obtain the required heating rate of metal nanoparticles on a transparent substrate [28].

3 Theory of spectral hole burning in the inhomogeneously broadened absorption profile of metal nanoparticles

3.1 *General remarks*

Before we describe the model that allows us to extract the plasmon dephasing time in nanoparticles, several preconditions for the theoretical treatment will be mentioned briefly. Firstly, an inhomogeneous distribution of resonance frequencies of isolated clusters as a result of a certain size and/or shape distribution is not necessarily the only reason for large broadening of the linear extinction spectra. In fact, spectra of identical metal particles that are densely packed and interact via dipole fields may look very similar to the spectrum of an ensemble of non interacting particles with a broad size or shape distribution [2, 33]. However, if the width of the extinction spectrum is mainly due to the interaction between the particles, there is obviously no possibility to selectively deplete a narrow part of the whole spectrum. Conversely, observation of hole burning in our experiments furnishes clear evidence of inhomogeneously broadened and non-interacting particles. Scanning force microscopy images of the supported metal clusters support this conclusion [28, 29]. Secondly, in view of the thermal constants of the dielectric substrate as well as the nanometer-size of the metal particles, laser illumination leads to a highly selective temperature distribution over the substrate surface. Since the substrate does not absorb laser light, it is heated only through the energy flow originating from the clusters, see Fig. 2. The heat diffusion length in a metal is much larger than the cluster size; therefore, each cluster is heated almost homogeneously and may be regarded as a point source of heat located on the substrate surface. The three-dimensional heat flow from a single nanoparticle is known to lead to a saturation of the temperature rise, the maximum value being reached during the laser pulse [34, p. 47]. In contrast, the heat diffusion length in the substrate is smaller than the mean distance between the clusters; hence, the clusters do not heat each other appreciably. Nevertheless, this small effect may be accounted for by an average temperature rise due to the one dimensional heat flow [34, p. 42], [35, p. 75] from the whole illuminated area into the interior of the substrate. Finally, the spectral bandwidth of the applied laser light is so small as compared to the involved homogeneous and inhomogeneous widths of the plasmon transition that it can be ignored.

The model to be described in the following sections consists of four steps:

1. Computation of the optical absorption spectrum of the nanoparticles as grown with a size and shape distribution, i.e. inhomogeneous line broadening
2. Calculation of the temperature rise induced by absorption of laser light
3. Calculation of the evaporation rate of atoms from the surfaces of the nanoparticles and of their dimensions after selective laser heating
4. Computation of the optical spectrum of the modified distribution and of the difference of the spectra after and before laser irradiation, i.e. of the shape of the spectral hole and its width.

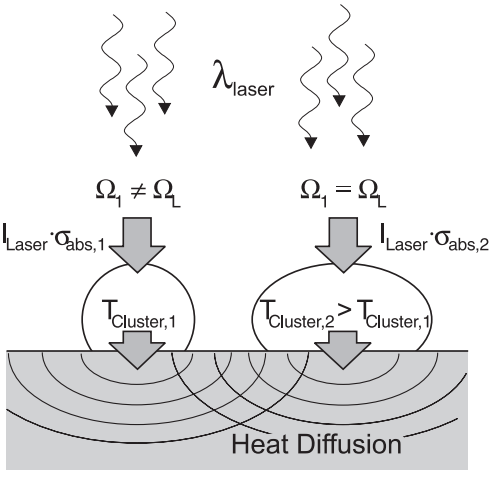

FIGURE 2 Scheme of the energy deposition and redistribution in an ensemble of supported metal nanoparticles on a transparent substrate during the thermally induced hole burning process

3.2 *Theoretical treatment of spectral hole burning*

The extinction cross section of a small metal particle depends on its size as well as on its shape. There are two important simplifications of this dependence for particles in the size range of up to several tens of nanometers. Firstly, for such particle sizes the quasistatic approximation can be applied, and the optical extinction is mainly due to absorption, the absorption cross section being directly proportional to the particle volume [30, p. 140, p. 145]. Secondly, the spectral dependence of the absorption cross section is determined only by the particle shape and is independent of its volume. Careful analysis of the extinction spectra in combination with atomic force microscopy shows that the particles can be described as oblate, rotational ellipsoids with two main axes a and b, the smaller one, a, being perpendicular to the surface plane. Each particle possesses two resonance frequencies, corresponding to plasmon excitations parallel and perpendicular to the surface [30, p. 141 ff.]. The values of these resonance frequencies depend solely on the axial ratio a/b [30, p. 141 ff.]. For s-polarized light only the low frequency (1,1)-mode contributes to the extinction spectrum. Hence, there is a one to one correspondence between the particle shape and its resonance frequency. Moreover, the strong correlation between the size and the shape of the particles as observed experimentally [28, 29] gives us the possibility of classifying the whole particle ensemble by the resonance frequency Ω, the particle volume V being a function of Ω. The absorption cross section of a particle with resonance frequency Ω and volume V at any particular frequency Ω will be denoted as $\sigma(\omega, \Omega)$. If we assume that the metal may be characterized by a frequency dependent complex dielectric function $\varepsilon = \varepsilon_1 + \mathrm{i}\varepsilon_2$, the quasistatic formula for $\sigma(\omega, \Omega)$ reads as

$$\sigma(\omega, \Omega) = \frac{V\omega}{c} \frac{[1-\varepsilon_1(\Omega)]^2\, \varepsilon_2(\omega)}{[\varepsilon_1(\Omega)-\varepsilon_1(\omega)]^2 + \varepsilon_2^2(\omega)} \tag{1}$$

where c is the speed of light. For Drude-like metals with bulk plasma frequency ω_p and damping constant γ, the dielectric function has the explicit analytical form

$$\varepsilon(\omega) = 1 - \frac{\omega_\mathrm{p}^2}{\omega(\omega + \mathrm{i}\gamma)} \tag{2}$$

and (1) simplifies to

$$\sigma(\omega, \Omega) = \frac{V\gamma\omega_\mathrm{p}^2}{4c} \frac{1}{(\omega-\Omega)^2 + (\gamma/2)^2}\,, \tag{3}$$

provided $\gamma \ll \Omega$ and $|\omega - \Omega| \ll \Omega$. In this case, the spectral dependence of the absorption cross section is a Lorentzian, the width and amplitude of which are independent of the particle resonance frequency. This suggests a widely accepted interpretation of surface plasmon excitation as a damped harmonic oscillator. This interpretation may be extended to real metals with dielectric functions rather different from (2) if one defines the frequency dependent width of the plasmon resonance as follows [2]:

$$\Gamma_\Omega = \frac{2\varepsilon_2(\Omega)}{|\,[\mathrm{d}\varepsilon_1(\omega)/\mathrm{d}\omega]_{\omega=\Omega}\,|} \tag{4}$$

and its strength

$$\sigma^0(\Omega) = \frac{V\Omega}{c} \frac{[1-\varepsilon_1(\Omega)]^2}{\varepsilon_2(\Omega)}\,. \tag{5}$$

Then, in close proximity of the plasmon frequency Ω, (1) may be written as

$$\sigma(\omega, \Omega) = \sigma^0(\Omega) \frac{(\Gamma_\Omega/2)^2}{(\omega-\Omega)^2 + (\Gamma_\Omega/2)^2}\,. \tag{6}$$

This is similar to (3) except that the spectral width and strength of the plasmon resonance now depend on the plasmon resonance frequency which, in turn, is defined by the particle shape. Using (6) is justified as long as Γ_Ω does not vary too much when Ω changes by $\pm\Gamma_\Omega$, i.e. $|\Gamma_{\Omega\pm\Gamma_\Omega} - \Gamma_\Omega| \ll \Gamma_\Omega$. This condition definitely breaks down when $\varepsilon_1(\Omega)$ reaches its maximum and Γ_Ω defined by (4) tends to infinity.

Equation (6) may be further generalized by substituting Γ_Ω of (4) by the more general parameter $\Gamma_\mathrm{hom}(\Omega)$. It is larger than Γ_Ω and allows for all damping mechanisms like quantum size effects, chemical interface damping, etc., as well as for the damping already included in (4). Now, the absorption spectrum of the whole ensemble is given by

$$S_1(\omega) = \int f(\Omega)\sigma(\omega, \Omega)\mathrm{d}\Omega\,, \tag{7}$$

$f(\Omega)$ being the inhomogeneous distribution of the plasmon frequencies due to the shape distribution of the particles. Substituting (6) for $\sigma(\omega, \Omega)$ in (7), one obtains the final form of the absorption spectrum of the nanoparticles before laser treatment

$$S_1(\omega) = \int f(\Omega)\sigma^0(\Omega) \frac{(\Gamma_\mathrm{hom}(\Omega)/2)^2}{(\omega-\Omega)^2 + (\Gamma_\mathrm{hom}(\Omega)/2)^2}\mathrm{d}\Omega\,. \tag{8}$$

As the next step the temperature rise of the nanoparticles during the laser pulse was calculated under the assumption that the absorbed photon energy is totally converted into heat. When a several nanometer large metal particle on a transparent support is illuminated with a laser pulse of several nanoseconds duration its temperature rise can be very well estimated if it is treated as a point source of heat on the infinite substrate in steady state. The temperature rise of a cluster with resonance frequency Ω induced by the laser radiation with frequency Ω_L and fluence F is $C_\Omega F\sigma(\Omega_L, \Omega)$, where C_Ω is a constant determined by the thermal conductivity of the substrate λ and by the radius R_Ω of the contact area between the cluster and the substrate:

$$C_\Omega = \frac{1}{\pi\lambda R_\Omega \tau}\,, \tag{9}$$

where τ is the laser pulse duration. The temperature during illumination is

$$T(\Omega) = T_0 + C_\Omega F\sigma(\Omega_L, \Omega)\,, \tag{10}$$

T_0 being the initial sample temperature before illumination.

When the temperature rise is large enough, different thermally activated processes may lead to changes of the particle

resonance frequency and the strength of the resonance. We consider evaporation of atoms first. The rate of atom evaporation and the resulting variations of the volume and the axial ratio of the clusters are proportional to $\exp[-E_a/k_{\mathrm{B}}T(\Omega)]$, where E_a is the activation energy for evaporation and k_{B} the Boltzmann constant. Assuming first order evaporation kinetics with a pre exponential factor v of the order of the vibrational frequency $10^{12}\ \mathrm{s}^{-2}$ we obtain

$$\frac{\mathrm{d}\sigma^0(\Omega)}{\mathrm{d}t} = -v\sigma^0(\Omega)\exp\left[-E_a/k_{\mathrm{B}}T(\Omega)\right] . \tag{11}$$

In what follows we will restrict ourselves to short illumination times τ, which results in rather small changes of the particle volume. Then, the overall change of $\sigma^0(\Omega)$ is

$$\delta\sigma^0(\Omega) = -a(\Omega)\exp\left[-E_a/k_{\mathrm{B}}T(\Omega)\right] , \tag{12}$$

where $a(\Omega) = v\tau\sigma^0(\Omega)$ varies with Ω much more slowly than the exponential function. As outlined above, reduction of the particle size is accompanied by a change of its shape, so that the resonance frequency after laser treatment is shifted from its original position by some amount $\delta\Omega$. To account for a possible contribution of surface diffusion and to preserve the generality of the theoretical model we assume that the activation energy for shape changes, E_b, may be quite different from E_a. Hence, $\delta\Omega$ should be written as

$$\delta\Omega = b(\Omega)\exp\left[-E_b/k_{\mathrm{B}}T(\Omega)\right] , \tag{13}$$

where $b(\Omega)$ is a slowly varying function of Ω, as compared to the exponential function. Substituting the new values of the resonance frequency and the corresponding absorption cross section in (8), we obtain for the absorption spectrum after laser treatment

$$S_2(\omega) = \int f(\Omega)\left[\sigma^0(\Omega)+\delta\sigma^0(\Omega)\right] \times \frac{(\Gamma_{\mathrm{hom}}(\Omega)/2)^2}{(\omega-\Omega-\delta\Omega)^2+(\Gamma_{\mathrm{hom}}(\Omega)/2)^2}\mathrm{d}\Omega . \tag{14}$$

The shape of the spectral hole is determined as the difference between the absorption spectra after and before the laser treatment:

$$\delta S(\omega) = S_2(\omega) - S_1(\omega) . \tag{15}$$

To facilitate the comparison with the experimental results this expression will be further simplified in the following section.

3.3 *Analytical expression for the profile of the spectral hole*

Expanding (14) to the first order in small changes $\delta\sigma^0(\Omega)$ and $\delta\Omega$, we obtain

$$\delta S(\omega) = \delta S_a(\omega) + \delta S_b(\omega) , \tag{16}$$

where

$$\delta S_a(\omega) = \int f(\Omega)\frac{\delta\sigma^0(\Omega)\,(\Gamma_{\mathrm{hom}}(\Omega)/2)^2}{(\omega-\Omega)^2+(\Gamma_{\mathrm{hom}}(\Omega)/2)^2}\mathrm{d}\Omega \tag{17}$$

and

$$\delta S_b(\omega) = \int f(\Omega)\frac{2(\omega-\Omega)\sigma^0(\Omega)\,(\Gamma_{\mathrm{hom}}(\Omega)/2)^2\,\delta\Omega}{\left[(\omega-\Omega)^2+(\Gamma_{\mathrm{hom}}(\Omega)/2)^2\right]^2}\mathrm{d}\Omega . \tag{18}$$

To make the next step, closer examination of the exponential function in (12) and (13) is required. Let us consider (12) first. We introduce the dimensionless quantities θ_{0a} and θ_{La}:

$$\theta_{0a} = \frac{k_{\mathrm{B}}T_0}{E_a} , \quad \theta_{La} = \frac{k_{\mathrm{B}}C_\Omega F\sigma^0(\Omega)}{E_a} , \tag{19}$$

which correspond to the initial temperature of the sample and the maximum temperature rise for particles illuminated at the resonance frequency; one obtains the following expression

$$\exp\left[-E_a/k_{\mathrm{B}}T(\Omega)\right] = \exp\left[-\frac{1}{\theta_{0a}+\theta_{La}\frac{1}{1+(\Omega-\Omega_L)^2/(\Gamma_{\mathrm{hom}}(\Omega)/2)^2}}\right] . \tag{20}$$

This function reaches its maximum value of

$$\exp\left[-\frac{1}{\theta_{0a}+\theta_{La}}\right] \tag{21}$$

for $\Omega = \Omega_L$. As θ_{0a} is assumed to be much smaller than unity and θ_{La} is of the order of θ_{0a} or larger, the exponential function in (20) falls very rapidly for $\Omega \neq \Omega_L$. The effective width of the region where it has values comparable with its maximum value (21) may be described by the inequality

$$|\Omega-\Omega_L| < \Delta_{La} , \tag{22}$$

where

$$\Delta_{La} = \frac{\theta_{La}+\theta_{0a}}{\sqrt{\theta_{La}}}\left(\Gamma_{\mathrm{hom}}\left(\Omega_L\right)/2\right) . \tag{23}$$

In this region (20) simplifies to

$$\exp\left[-E_a/k_{\mathrm{B}}T(\Omega)\right] = \exp\left[-\frac{1}{\theta_{0a}+\theta_{La}}\right]\exp\left[-\frac{(\Omega-\Omega_L)^2}{\Delta_{La}^2}\right] , \tag{24}$$

where Δ_{La} represents the half width of the Gaussian function at the level of $\exp(-1)$. Substitution of (24) into (12) and (17) leads to

$$\delta S_a(\omega) = \int \bar{A}(\Omega)\frac{\exp\left(-\frac{(\Omega-\Omega_L)^2}{\Delta_{La}^2}\right)(\Gamma_{\mathrm{hom}}(\Omega)/2)^2}{(\omega-\Omega)^2+(\Gamma_{\mathrm{hom}}(\Omega)/2)^2}\mathrm{d}\Omega , \tag{25}$$

where

$$\bar{A}(\Omega) = f(\Omega)a(\Omega)\exp\left(-\frac{1}{\theta_{0a}+\theta_{La}}\right) . \tag{26}$$

Following the same steps one obtains

$$\delta S_b(\omega) = \int \bar{B}(\Omega) \frac{\exp\left(-\frac{(\Omega-\Omega_L)^2}{\Delta_{Lb}^2}\right)(\omega-\Omega)\,(\Gamma_{\hom}(\Omega)/2)^2}{\left[(\omega-\Omega)^2+(\Gamma_{\hom}(\Omega)/2)^2\right]^2}\mathrm{d}\Omega\,, \quad (27)$$

where

$$\bar{B}(\Omega) = 2f(\Omega)\sigma^0(\Omega)b(\Omega)\exp\left(-\frac{1}{\theta_{0b}+\theta_{Lb}}\right) \quad (28)$$

and

$$\theta_{0b} = \frac{k_{\mathrm{B}}T_0}{E_b}\,, \quad \theta_{Lb} = \frac{k_{\mathrm{B}}C_\Omega F\sigma^0(\Omega)}{E_b}\,,$$
$$\Delta_{Lb} = \frac{\theta_{Lb}+\theta_{0b}}{\sqrt{\theta_{Lb}}}\,(\Gamma_{\hom}(\Omega_L)/2) \quad (29)$$

are defined in full analogy to (19), (23) and (26).

As long as Δ_{La} and Δ_{Lb} are so small that all other functions in (25) and (27) may be regarded as constant and taken out of the integral, these equations simplify to

$$\delta S_a(\omega) = -\sqrt{\pi}\Delta_{La}\bar{A}(\Omega_L)\,\frac{(\Gamma_{\hom}(\Omega_L)/2)^2}{(\omega-\Omega_L)^2+(\Gamma_{\hom}(\Omega_L)/2)^2}\,, \quad (30)$$

and

$$\delta S_b(\omega) = \sqrt{\pi}\Delta_{Lb}\bar{B}(\Omega_L)\,\frac{(\omega-\Omega_L)\,(\Gamma_{\hom}(\Omega_L)/2)^2}{\left[(\omega-\Omega_L)^2+(\Gamma_{\hom}(\Omega_L)/2)^2\right]^2}\,, \quad (31)$$

Summing up both contributions to (16) we finally obtain

$$\delta S(\omega) = -\tilde{A}\frac{(\Gamma_{\hom}(\Omega_L)/2)^2}{(\omega-\Omega_L)^2+(\Gamma_{\hom}(\Omega_L)/2)^2} + \tilde{B}\frac{(\omega-\Omega_L)\,(\Gamma_{\hom}(\Omega_L)/2)^3}{\left[(\omega-\Omega_L)^2+(\Gamma_{\hom}(\Omega_L)/2)^2\right]^2}\,, \quad (32)$$

where $\tilde{A}$ and $\tilde{B}$, which may be readily obtained from (30) and (31), are independent of ω.

It is essential to note that, contrary to the conventional hole burning techniques, this spectral hole consists of two contributions of different parity. The first, even term of (30) describes the spectral changes induced by the overall shrinking of the resonantly excited nanoparticles; the second, odd term represents the changes brought about by the increase of the axial ratio. $\tilde{A}$ and $\tilde{B}$ reflect the relative importance of both processes. Another peculiarity of the thermal mechanism of hole burning as used here is that the width of the spectral hole is equal to the width of the individual resonance, although in classical hole burning it is doubled. This is a consequence of the enhanced selectivity of the thermally activated process (24). As long as the laser fluence is low enough the width of the hole in the frequency distribution function is much narrower than the homogeneous width of the resonance. Hence, the width of the spectral hole described in the limit of low fluences by (32) is equal to the homogeneous width.

3.4 *Fluence broadening of spectral holes*

When the laser fluence rises the spectral hole broadens since the temperature rise of particles with neighboring axial ratios not fully in resonance with the laser gains importance as more and more energy is absorbed in the wings of their plasmon profiles. Formally, (32) holds for the limit when the widths Δ_{La} and Δ_{Lb} are much smaller than $\Gamma_{\hom}(\Omega_L)$. In reality, however, these widths can not be made arbitrarily small. According to (23) the ratio $\Delta_{La}/\Gamma_{\hom}(\Omega_L)$ reaches its minimum value of $\sqrt{\theta_{0a}}$, when $\theta_{La} = \theta_{0a}$. Moreover it may be desirable, from the experimental point of view, to use larger fluences than given by this relation to obtain better signals. When the power broadening of the spectral hole is known, it may be used to extrapolate the width to zero fluence and thus obtain the homogeneous width of the plasmon resonance even though the measurements were carried out under conditions of non negligible fluence broadening. Hence, the integrals in (25) and (27) should be computed more accurately to include the effects of the finite width of the Gaussian functions. At this point it is desirable to account also for the frequency dependence of other factors entering the integrands in (25) and (27), namely $\bar{A}(\Omega)$ and $\bar{B}(\Omega)$. As these terms are assumed to vary rather slowly, their frequency dependence may be modeled by Gaussian functions with central frequencies Ω_{0A} and Ω_{0B} and widths Δ_{0A} and Δ_{0B}

$$\bar{A}(\Omega) = \bar{A}(\Omega_L)\,\exp\left(\frac{(\Omega_L-\Omega_{0A})^2}{\Delta_{0A}^2}\right) \times \exp\left(-\frac{(\Omega-\Omega_{0A})^2}{\Delta_{0A}^2}\right) \quad (33)$$

and

$$\bar{B}(\Omega) = \bar{B}(\Omega_L)\exp\left(\frac{(\Omega_L-\Omega_{0B})^2}{\Delta_{0B}^2}\right) \times \exp\left(-\frac{(\Omega-\Omega_{0B})^2}{\Delta_{0B}^2}\right)\,. \quad (34)$$

The reason for this choice is that the product of two Gaussian functions may be represented as one Gaussian function. The width and the central frequency of this new Gaussian function are given by

$$\Omega_A = \Omega_L + (\Omega_{0A}-\Omega_L)\,\frac{\Delta_{La}^2}{\Delta_{La}^2+\Delta_{0A}^2} \quad \text{and} \quad \Delta_A^2 = \frac{\Delta_{La}^2\Delta_{0A}^2}{\Delta_{La}^2+\Delta_{0A}^2} \quad (35)$$

in the case of (25) and by

$$\Omega_B = \Omega_L + (\Omega_{0B}-\Omega_L)\,\frac{\Delta_{Lb}^2}{\Delta_{Lb}^2+\Delta_{0B}^2} \quad \text{and} \quad \Delta_B^2 = \frac{\Delta_{Lb}^2\Delta_{0B}^2}{\Delta_{Lb}^2+\Delta_{0B}^2} \quad (36)$$

in the case of (27). With these definitions we have

$$\delta S_a(\omega) = A^* \int \frac{\exp\left(-\frac{(\Omega-\Omega_A)^2}{\Delta_A^2}\right)(\Gamma_{\rm hom}(\Omega)/2)^2}{(\omega-\Omega)^2+(\Gamma_{\rm hom}(\Omega)/2)^2}\mathrm{d}\Omega \qquad (37)$$

and

$$\delta S_b(\omega) = B^* \int \frac{\exp\left(-\frac{(\Omega-\Omega_B)^2}{\Delta_B^2}\right)(\omega-\Omega)\,(\Gamma_{\rm hom}(\Omega)/2)^3}{\left[(\omega-\Omega)^2+(\Gamma_{\rm hom}(\Omega)/2)^2\right]^2}\mathrm{d}\Omega\,. \qquad (38)$$

For simplicity and clarity, the explicit formulations of A^* and B^* that are independent of ω will not be given here, although they may be obtained in a straightforward manner. The integral in (37) resembles a Voigt spectral line shape. It can be expressed in terms of the plasma dispersion function [36]. The same is true for (38). For small values of $\Delta_A/\Gamma_{\rm hom}$ and $\Delta_B/\Gamma_{\rm hom}$ the spectral shapes of $\delta S_a(\omega)$ and $\delta S_b(\omega)$ do not deviate considerably from (30) and (31), respectively, so that $\delta S(\omega)$ may be expressed in almost the same form as (32)

$$\delta S(\omega) = -A\frac{(\gamma_a/2)^2}{(\omega-\Omega_A)^2+(\gamma_a/2)^2} + B\frac{(\omega-\Omega_B)\,(\gamma_b/2)^3}{\left[(\omega-\Omega_B)^2+(\gamma_b/2)^2\right]^2}\,, \qquad (39)$$

where A and B may be expressed through A^* and B^*, correspondingly. The apparent widths γ_a and γ_b of the even and odd profiles contributing to (39) are different from the homogeneous width $\Gamma_{\rm hom}(\Omega_L)$ of the plasmon by small quantities that are proportional to Δ_A and Δ_B:

$$\gamma_a = \Gamma_{\rm hom}\left(1+\frac{3}{4}\frac{\Delta_A^2}{(\Gamma_{\rm hom}/2)^2}\right),$$

$$\gamma_b = \Gamma_{\rm hom}\left(1+\frac{3}{2}\frac{\Delta_B^2}{(\Gamma_{\rm hom}/2)^2}\right), \qquad (40)$$

Equations (39) and (40) together with (23) and (29) constitute the theoretical background for fitting the spectral holes and evaluation of $\Gamma_{\rm hom}(\Omega_L)$.

4 Experimental

For the experiments described in this article, Ag nanoparticles were prepared under UHV conditions by deposition of atoms on a sapphire substrate at room temperature. As a consequence oblate shaped clusters were generated by surface diffusion and nucleation of the adsorbed atoms [29]. In order to tune the dependence of the axial ratio of the particles on the size and to shift the maximum of the inhomogeneous distribution into a predetermined position, the sample was irradiated with ns laser pulses during the growth process. As a light source, the second harmonic of a Nd:YAG laser ($\lambda = 532$ nm) was used at a pulse fluence of 160 mJ/cm^2, the pulse duration being 7 ns. The laser system was operated at a repetition rate of 10 Hz and the angle of incidence of the p polarized light was set to 45°. Further details of the sample preparation are given in [28, 37]. As a result, by deposition of 15×10^{15} atoms/cm^2, measured using a quartz crystal microbalance, a particle ensemble with a mean radius of $\langle r\rangle = 10$ nm was formed.

The mean axial ratio of the spheroidally shaped aggregates was deduced from the position of the low energy (1,1)-mode surface plasmon resonance and comparison with calculations using the quasistatic approximation [30, p. 141 ff.] and the optical constants of [38]. For measurement of the absorption spectra before and after laser irradiation, the s-polarized light of a Xe-arc lamp was used in combination with a monochromator, the angle of incidence on the substrate being 45°. After preparation the optical spectra of the particles reveal a resonance position of the (1,1)-mode of 2.91 eV corresponding to a mean axial ratio of 0.47, see Fig. 3.

For spectral hole burning the particles were irradiated using the light of a BBO OPO that was pumped by the third harmonic of the Nd:YAG laser. The pulse duration of the OPO was specified at 2–4 ns and again the laser system was operated at a repetition rate of 10 Hz. In order to optimize the interaction between laser light and particles, the photon energy of the OPO was tuned almost to the maximum of the inhomogeneously broadened plasmon resonance of the cluster ensemble, i.e. 2.93 eV. In subsequent steps the particles were irradiated with 100 laser pulses using seven different laser fluences evenly distributed between 20 and 50 mJ/cm^2, the optical spectra being measured between subsequent steps, see Fig. 3.

Figure 4 displays the difference of the absorption spectra measured after and before irradiation with 100 laser pulses of a fluence of 30 mJ/cm^2 (open circles). An asymmetrical hole is produced in the vicinity of the laser frequency. It shows a minimum of -1.3% at 2.85 eV that is followed by an increase of absorption with a maximum of 0.75% at 3.05 eV. Similar curves are obtained for the other fluences. Our theoretical model (39) reproduces the shape of the generated hole quite nicely. It was found also that the number of variable parameters may be further reduced by setting $\gamma_a = \gamma_b = \gamma$ and $\Omega_a = \Omega_b$ without loss of quality of the

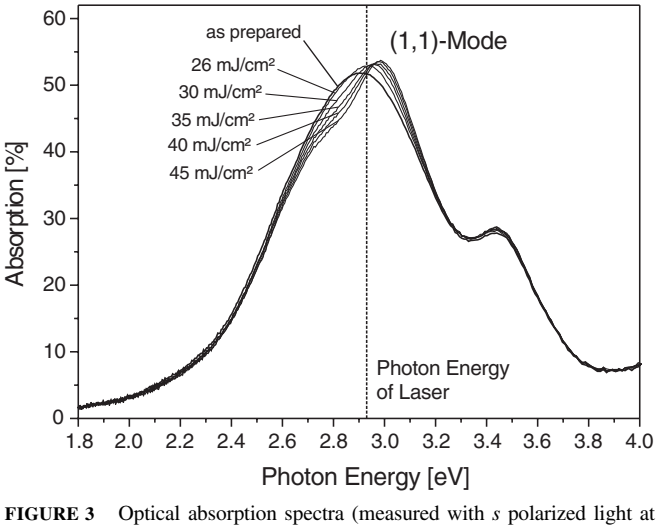

FIGURE 3 Optical absorption spectra (measured with s polarized light at an angle of incidence of 45°) before and after laser irradiation with 100 laser pulses at a photon energy of 2.93 eV and different fluences

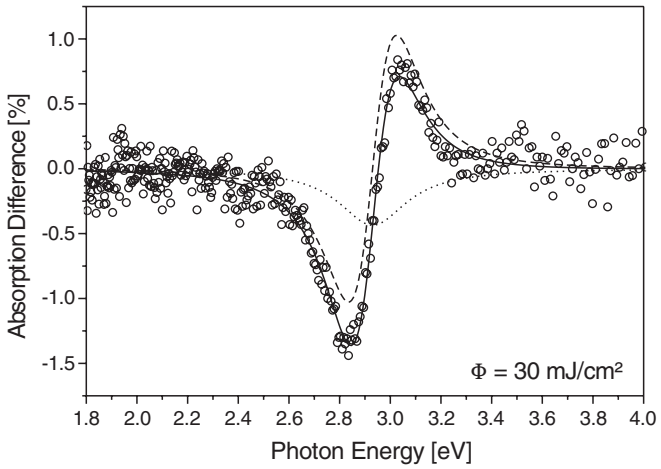

FIGURE 4 Difference of absorption after and before laser irradiation with 100 laser pulses at a fluence of 30 mJ/cm^2 (*open circles*). The *solid line* represents a fit to the theoretical model of (39). Separation of the theoretical curve into even (*dotted line*) and odd (*dashed line*) contributions is also shown

fit. Figure 4 plots such a fit as well as the even and odd contributions to the theoretical curve. The fluence dependence of γ obtained in this way is shown in Fig. 5. Linear dependence of γ on the laser fluence suggested by the experimental results may be obtained in the framework of the theoretical model described above under the following two additional assumptions. Firstly, we neglect the initial temperature T_0 of the surface as compared to the temperature rise during illumination. We further assume that the fluence broadening is considerably smaller than the inhomogeneous broadening even for the largest fluences used experimentally. These two assumptions lead to the conclusion that the fluence broadening is directly proportional to the fluence. Hence, linear extrapolation to zero fluence may be used to find the homogeneous line width. In the case presented above we obtain the homogeneous width $\Gamma_{\mathrm{hom}}(2.93\,\mathrm{eV}) = (230 \pm 20)$ meV that corresponds to a dephasing time of $T_2(2.93\,\mathrm{eV}) = (5.7 \pm 0.5)$ fs.

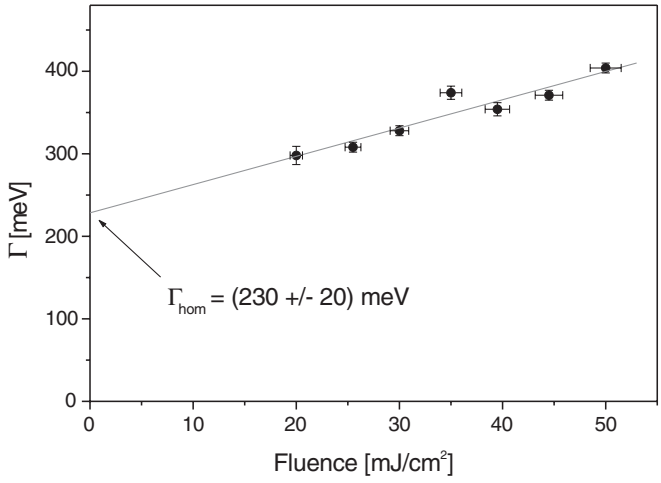

FIGURE 5 Fluence dependence of the apparent width of the difference spectra (*closed circles*). The homogeneous width is obtained via linear extrapolation to zero fluence (*solid line*)

5 Conclusions

In summary, we have developed and verified experimentally a theoretical model that quantitatively reproduces the spectral hole shapes as well as their dependence on the applied laser fluence. With this tool at hand the dephasing times of the surface plasmon excited in the nanoparticles may be readily obtained despite the large inhomogeneous broadening inherent in many methods of sample preparation. Hence a new possibility to study the ultrafast electron dynamics in small metal particles opens up.

ACKNOWLEDGEMENTS Financial support of the Fond der Chemischen Industrie is gratefully acknowledged. One of the authors (T.V., State Optical Institute, St. Petersburg, Russia) is grateful to DAAD for a scholarship.

REFERENCES

1 F. Stietz, J. Bosbach, T. Wenzel, T. Vartanyan, A. Goldmann, F. Träger: Phys. Rev. Lett. **84**, 5644 (2000)
2 U. Kreibig, M. Vollmer: *Optical Properties of Metal Clusters* (Springer Ser. Mater. Sci. 25) (Springer, Berlin 1995)
3 B. Messinger, K.U. von Raben, R. Chang, P. Barber: Phys. Rev. B **24**, 649 (1981)
4 S. Grésillon, L. Aigouy, A. Boccara, J. Rivoal, X. Quelin, C. Desmarest, P. Gadenne, V. Shubin, A. Sarychev, V. Shalaev: Phys. Rev. Lett. **82**, 4520 (1999)
5 K.S.G. Chumanov, M. Cotton: Anal. Chem. **70**, 3898 (1998)
6 S. Nie, S. Emory: Science **275**, 1102 (1997)
7 A. Wokaun: Mol. Phys. **56**, 1 (1985)
8 R. Haglund, Jr., L. Yang, R. Magruder, III, J. Wittig, K. Becker, R. Zuhr: Opt. Lett. **18**, 373 (1993)
9 T. Schalkhammer: Chem. Mon. **129**, 1067 (1998)
10 L. Novotny, R. Bian, X. Xie: Phys. Rev. Lett. **79**, 645 (1997)
11 V. Halté, J. Guille, J. C. Merle, I. Perakis, J. Y. Bigot: Phys. Rev. B **60**, 11 738 (1999)
12 C. Voisin, N.D. Fatti, D. Christofilos, F. Vallée: J. Phys. Chem. **105**, 2264 (2001)
13 S. Stagira, M. Nisoli, S.D. Silvestri, A. Stella, P. Tognini, P. Cheyssac, R. Kofman: Chem. Phys. **251**, 259 (2000)
14 M. Perner, P. Bost, U. Lemmer, G. von Plessen, J. Feldmann, U. Becker, M. Mennig, M. Schmitt, H. Schmitt: Phys. Rev. Lett. **78**, 2192 (1997)
15 F. Calvayrac, P. Reinhard, E. Suraud, C. Ullrich: Phys. Rep. **337**, 493 (2000)
16 T. Klar, M. Perner, S. Grosse, G. von Plessen, J. Feldmann: Phys. Rev. Lett. **80**, 4249 (1998)
17 C. Sönnichsen, S. Geier, N. Hecker, G. von Plessen, J. Feldmann, H. Ditlbacher, B. Lamprecht, J. Krenn, F. Aussenegg, V. H. Chan, J. Spatz, M. Möller: Appl. Phys. Lett. **77**, 2949 (2000)
18 N. Nilius, N. Ernst, H. J. Freund: Phys. Rev. Lett. **84**, 3994 (2000)
19 M. Simon, F. Träger, A. Assion, B. Lang, S. Voll, G. Gerber: Chem. Phys. Lett. **296**, 579 (1998)
20 B. Lamprecht, J. Krenn, A. Leitner, F. Aussenegg: Phys. Rev. Lett. **83**, 4421 (1999)
21 B. Lamprecht, A. Leitner, F. Aussenegg: Appl. Phys. B **68**, 419 (1999)
22 Y. H. Liau, A.N. Unterreiner, Q. Chang, N.F. Scherer: J. Phys. Chem. B **105**, 2135 (2001)
23 D. Pines, P. Nozières: *The Theory of Quantum Liquids* (Benjamin, New York 1966)
24 U. Kreibig, M. Gartz, A. Hilger: Ber. Bunsenges. Phys. Chem. **101**, 1593 (1997)
25 B. Persson: Surf. Sci. **281**, 153 (1993)
26 B. Lamprecht, J. Krenn, A. Leitner, F. Aussenegg: Appl. Phys. B **69**, 223 (1999)
27 T. Vartanyan, M. Simon, F. Träger: Appl. Phys. B **68**, 425 (1999)
28 F. Stietz: Appl. Phys. A **72**, 381 (2001)
29 T. Wenzel, J. Bosbach, F. Stietz, F. Träger: Surf. Sci. **432**, 257 (1999)
30 C.F. Bohren, D.R. Huffman: *Absorption and Scattering of Light by Small Particles* (Wiley, New York 1983)
31 H. de Vries, D.A. Wiersma: Phys. Rev. Lett. **36**, 91 (1976)

32 A. Müller, W. Richter, L. Kador: Chem. Phys. Lett. **285**, 92 (1998)
33 V. Russier, M.P. Pileni: Surf. Sci. **425**, 313 (1999)
34 A.M. Prokhorov, V.I. Konov, I. Ursu, I.N. Mihailescu: *Laser Heating of Metals* (IOP, Bristol 1990)
35 H.S. Carslaw, J.C. Jaeger: *Conduction of Heat in Solids,* 2nd edn. (Oxford Science, New York 1997)
36 B.D. Fried, S.D. Conte: *The Plasma Dispersion Function* (Academic, New York, London 1961)
37 T. Wenzel, J. Bosbach, A. Goldmann, F. Stietz, F. Träger: Appl. Phys. B **69**, 513 (1999)
38 D. Edward, I. Palik: *Handbook of Optical Constants of Solids* (Academic, Orlando, Florida 1985)